



32  
33  
34  
35  
36  
37  
38  
39  
40  
41  
42  
43  
44  
45  
46  
47  
48  
49  
50  
51  
52  
53  
54  
55  
56  
57  
58  
59  
60

## Abstract

Coronaviruses remodel intracellular membranes to form specialized viral replication compartments, such as double-membrane vesicles where viral RNA genome replication takes place. Understanding the factors affecting host response is instrumental to design of therapeutics to prevent or ameliorate the course of infection.

As part of explorative tests in hospitalized patients with confirmed COVID-19 infection participating in ODYSSEY trial, we obtained samples for whole genome sequencing analysis as well as for viral genome sequencing. Based on our data, we confirm one of the strongest severity susceptibility locus thus far reported in association with severe COVID-19: 3p21.31 locus with lead variant rs73064425. We further examine the associated region. Interestingly based on LD analysis we report 3 coding mutations within one gene in the region of FYVE and Coiled-Coil Domain Autophagy Adaptor 1 (*FYCO1*). We specifically focus on the role of *FYCO1* modifiers and gain-of-function variants. We report the associations between the region and clinical characteristics in this severe set of COVID-19 patients.

We next analyzed expression profiles of *FYCO1* across all 466 compounds tested. We selected only those results that showed a significant reduction of expression of *FYCO1*. The most significant candidate was indomethacin – an anti-inflammatory that could potentially downregulate *FYCO1*. We hypothesize that via its direct effects on efficiency of viral egress, it may serve as a potent therapeutic decreasing the replication and infectivity of the virus. Clinical studies will be needed to examine the therapeutic utility of indomethacin and other compounds downregulating *FYCO1* in COVID-19 infection and other strains of betacoronaviruses.

**Keywords:** COVID-19, therapeutics, whole genome sequencing, viral genetics, blocking viral egress

## 61 **Introduction**

62 The emergence of highly pathogenic zoonotic viruses calls for further research in order to  
63 understand, treat and ideally prevent such infections ultimately circumventing epidemics.

64 Currently accurate prognoses are confounded by our inability to predict disease severity and  
65 virulence across space and time. Virus-human interactions have driven around 30% of the human  
66 genome evolution since divergence from chimpanzee. Different variants, genes affect severity to  
67 a range of infections, for example: *IFITM3*, *IRF7* in influenza, *SFPA/D* and *VTR* in RSV, *CCR5*  
68 in HIV, *IFNG* in HTVL-1 and *TNF* in HPV to name a few. The complex interplay between  
69 environmental, viral, and host genetic factors drives differences in individual disease  
70 progression, severity, and outcome results. Understanding resilience and susceptibility factors  
71 should enable one to design prophylactics and therapeutics.

72

73 SARS-CoV-2 is a novel coronavirus that has led to a worldwide pandemic<sup>1</sup>. There is a  
74 high mortality rate associated with the virus and despite measures implemented to contain the  
75 spread of the virus, over xx were reported. The ACE2 binding affinity with RBD on the Spike  
76 protein of SARS-CoV-2 is 10-20x higher than that of the SARS-CoV. The clinical spectrum of  
77 this disease is heterogeneous, and infected individuals viral RNA shedding pattern differ across  
78 individuals at baseline. Similarly to other positive-sense RNA viruses, coronaviruses remodel  
79 intracellular membranes to form specialized viral replication compartments. Depending on the  
80 time course of the infection, the structure, composition, and formation of virus replication  
81 organelles appear to be varied and dynamic. Understanding the mode of action of this virus in  
82 the context of its interaction with the host genome is fundamental to the design of optimal  
83 therapeutic strategies.

84 In the early months of the epidemic it became apparent that advanced age and  
85 comorbidities are associated with higher risk for severe infection yet none of these fully explain  
86 the heterogeneous course of the infection amongst individuals<sup>2</sup>. To that end several sequencing  
87 projects have been commenced since the beginning of the epidemic. Initial results from COVID-  
88 19 initiative suggest a locus on chromosome 3p21.31, the peak association with severity of the  
89 disease, signal that has been observed by the Severe Covid-19 GWAS Group and further  
90 replicated by other host genome sequencing consortia<sup>3,4,5</sup> and the UKbiobank<sup>6</sup>. The genetic  
91 variants on chromosome 3 that are most associated with severe COVID-19 are all in high linkage

92 disequilibrium (LD). Furthermore recent phylogenetic analysis showed that the risk haplotype  
93 thus entered the modern human population from Neanderthals (Vindija 33.19 Neanderthal)<sup>7</sup>.  
94 Specifically, we focused on this region is because the 3p21.31 regional severity association was  
95 the strongest one replicated by multiple consortia including the COVID-19 initiative and latest  
96 Nature report by Casteneira et al., (rs73064425, OR=2.14, discovery p=4.77 × 10<sup>-30</sup>) (top  
97 variants can be accessed in the supplementary material)

98  
99 As part of explorative tests in hospitalized patients with confirmed SARS-CoV-2 positive  
100 infection participating in ODYSSEY trial, we obtained blood samples for whole genome  
101 sequencing analysis as well as nasopharyngeal swabs for further viral genome sequencing. We  
102 have conducted whole genome sequencing on first cohort participants as well as deep clinical  
103 phenotyping. Based on our data, we confirm one of the strongest susceptibility locus reported  
104 and now replicated with lead variant being rs73064425. We further examine the associated  
105 region, with specific focus on the role of *FYCO1* gene. We further discuss the associations  
106 between the region and clinical characteristics in this severe set of COVID-19 patients.

107  
108  
109

## 110 **Results**

### 111 ***Regional association***

112 We replicate the strongest susceptibility locus reported and now replicated is within, *3p21.31*  
113 *locus*, rs73064425 Leucine Zipper Transcription Factor Like 1 (LZTFL1) reported by Casteneira  
114 et al., as the strongest association with severity (rs73064425, OR=2.14, discovery  $p=4.77 \times 10^{-}$   
115 30). We replicate this association in our cohort of hospitalized patients (OR 3.2, CI  
116 1.8728 to 5.4637,  $p\text{-value}<0.0001$ ). The variant has a global gnomAD MAF of 0.05. We report  
117 an increased MAF 0.19 in ODYSSEY, and consistently with gnomAD, we report a MAF of 0.05  
118 in Vanda 2000 controls. The highest allelic frequency for this variant globally is present in  
119 Ashkenazi Jewish (MAF 0.12) and the lowest frequency is present amongst East and South  
120 Asian populations (MAF 0.0006). The GWAS signal covers a cluster of six genes (*SLC6A20*,  
121 *LZTFL1*, *CCR9*, *FYCO1*, *CXCR6*, and *XCRI*), several of which with functions that could be  
122 potentially relevant to Covid-19. The variant is a strong eQTL for CXCR6 and SLC6A20 in  
123 GTEX<sup>8</sup>. The locus itself is within a highly regulatory region, as an enhancer for Primary B cells  
124 from peripheral blood and modifier H3K4me1 in accordance with Haploreg. Furthermore the  
125 locus is associated with monocyte percentage (UK Biobank field: 30190-0.0) in Gene Atlas.  
126

127 Next we reconstructed LD to test if the signal (non-coding, top SNP by p-value) from  
128 other large studies can be reproduced and extended to nearby genes, Where are the “limits” of  
129 the signal on Odyssey data, Are there any coding variants. Interestingly there are 3 coding  
130 mutations within one gene in the region (*FYCO1*) causing 2 amino acid substitutions (two  
131 mutations within same codon, 1001, resulting in one missense mutation, third in strong LD). All  
132 3 coding variants are in strong LD with top SNPs published previously within the region and  
133 seem to be the strongest signal for our Odyssey samples. Having ~2000 control genomes we can  
134 see that all 3 coding variants form a strong LD. Quintessentially the risk is conveyed by the  
135 extent of existing LD structure in that region as shown in Supplementary Figures. Specifically,  
136 rs33910087 is an eQTL for CXCR6 and based on GeneAtlas, the genotyped variant is highly  
137 significant modifier of monocyte percentage ( $p=3.8479e-46$ ).

138

139 The association of the locus with severity of infection in interaction with SARS-CoV-2  
140 remains to be examined. Functionally *FYCO1* encodes a protein involved in vesicle transport and

141 autophagy. It has been suggested as a key mediator linking ER-derived double membrane  
142 vesicles, the primary replication site for coronaviruses, with the microtubule network<sup>9</sup>. *FYCO1*  
143 through its LC3-interacting region (LIR) motif was shown to be important for the fusion of  
144 autophagosomes with lysosomes. *FYCO1* dimerizes via the CC region, interacts with PI3P via  
145 its FYVE domain, and forms a complex with Rab7 via a part of the CC region located in front of  
146 the FYVE domain<sup>9</sup>. Specifically, *FYCO1* was shown to act as a Rab7 effector that binds to LC3  
147 and PI3P to mediate microtubule plus end-directed vesicle transport<sup>10</sup>. The depletion of Rab7  
148 inhibits maturation of late endosomes/MVBs and leads to reduced lysosome numbers in cells<sup>11</sup>.  
149 *FYCO1* also mediates clearance of  $\alpha$ -synuclein aggregates through a Rab7-dependent  
150 mechanism, overexpression reducing number of cell with  $\alpha$ -synuclein aggregates<sup>12</sup>. In another  
151 recent report authors perform a genome-scale CRISPR loss-of-function screen in human alveolar  
152 basal epithelial carcinoma cells to identify genes whose loss enabled resistance to SARS-CoV-2  
153 viral infection<sup>13</sup>. Loss of *RAB7A* reduces viral entry/egress by sequestering the ACE2 receptor  
154 inside cells<sup>13</sup>. Furthermore, depletion of *FYCO1* or antibodies against the N-terminus of LC3  
155 blocks the subcellular redistribution of autophagosomes<sup>14</sup>. Indeed, rare *FYCO1* variants some of  
156 which contain missense mutations in the LIR domain have recently been associated with  
157 inclusion body myositis a disease characterized by impaired autophagic degradation.

158  
159 We stipulate gain of function variants in *FYCO1* confer higher risk of severe course of  
160 COVID-19 induced infection and likely other betacoronaviruses. Temporarily downregulating  
161 *FYCO1* seems to be protective, hence the locus is likely crucial to designing therapeutic  
162 strategies for this and other strain of betacoronaviruses.

### 163 164 ***FYCO1* and drug-gene expression**

165 We have conducted a high throughput drug screen gene expression analysis to identify  
166 compounds that would downregulate the expression of *FYCO1*. To discover potential,  
167 pharmaceutical agents capable of affecting transcriptional expression levels of *FYCO1*  
168 implicated in SARS-CoV and SARS-CoV2 patho-physiology, we have screened 466 compounds  
169 belonging to 14 different therapeutic classes. Screening was conducted using human retinal  
170 pigment epithelia cell line (ARPE-19) and gene expression changes were collected across 12,490  
171 genes. We analyzed the expression profiles of *FYCO1* across all 466 compounds tested. In order

172 to find positive hits we selected only those results that showed a reduction of expression of  
173 *FYCO1* (1.5 -fold difference). The top significant candidate indomethacin is (displayed in **Table**  
174 **1**) a drug that has both anti-inflammatory and antiviral actions. Indomethacin was previously  
175 shown to have potent direct antiviral activity against the coronaviruses SARS-CoV and CCoV.  
176 Its potent antiviral activity (>1,000-fold reduction in virus yield) was previously confirmed in  
177 vivo in CCoV-infected dogs (Amici). These screens warrant further confirmatory tests  
178 nevertheless the strategy to weaken viral egress could be potentially useful for strains beyond  
179 SARS-CoV-2

180

<i>Compound</i>	<b>FYCO1</b> <b>Log2(treated)</b>	<b>FYCO1</b> <b>Log2(Ctrl)</b>	<b>FYCO1</b> <b>Log2( diff)</b>
<i>Indomethacin</i>	4.94	6.48	1.53
<i>Primidone</i>	6.44	7.94	1.49
<i>TriprolidineHydrochloride</i>	6.49	7.98	1.49
<i>Baclofen</i>	6.72	7.94	1.21

181

182 **Table 1.**

183

#### 184 ***Clinical Characteristics of carriers***

185 Both heterozygotes and homozygotes were severe hospitalized patients treated for COVID-19.  
186 The signal is one of severity however we wanted to check if the variant carriers would have any  
187 particular clinical characteristics. To that end we tested systemic cytokine panel in addition to  
188 standard lab tests. Clinical characteristics across genotypes are displayed in **Supplementary**  
189 **Material**. Noticeable is the linear distribution with higher sodium and chloride seen in  
190 homozygous individuals. All study patients met inclusion criteria included: age 18-90; confirmed  
191 laboratory COVID-19 infection; confirmed pneumonia by chest radiograph or computed  
192 tomography; fever defined as temperature  $\geq 36.6$  °C armpit,  $\geq 37.2$  °C oral, or  $\geq 37.8$  °C rectal  
193 since admission or the use of antipyretics; PaO<sub>2</sub> / FiO<sub>2</sub>  $\leq 300$ ; 6. in-patient hospitalization. We  
194 furthermore sequenced the viral genome sequence data in conjunction with host sequencing. We  
195 report coding mutations in SARS-CoV-2 based CoV-GLUE annotations<sup>15</sup>. All known variants  
196 reported in CoV-Glue<sup>15</sup> (until 11/23/2020) variants were annotated. As the viral strains evolved,  
197 the 614th aa position of the S protein, aspartate became replaced by glycine ultimately becoming

198 the ubiquitous strain, hence making open conformations more likely. All patients are carriers of  
199 the S:D614G variant - variant in the spike protein D614G that rapidly became dominant strain  
200 according to latest GISAID data<sup>16,17</sup>.

201

## 202 **Discussion**

203 Coronaviruses remodel intracellular membranes to form specialized viral replication  
204 compartments, such as double-membrane vesicles where viral RNA genome replication takes  
205 place. Understanding the formation and operation of these vesicles is instrumental to optimal  
206 design of therapeutics to prevent or ameliorate the course of infection. Here via findings from  
207 whole genome sequencing and association with severity of COVID-19, we were led to a locus  
208 that may in fact be functionally relevant in predisposing individuals to severe course of infection  
209 via its direct effects on efficiency of viral egress.

210

211 *FYCO1* has a direct link to formation of vesicles and autophagy. Pathogenic mutations in  
212 *FYCO1* can affect intracellular transport of autophagocytic vesicles. Depletion of *FYCO1* has  
213 been shown to block distribution of autophagosomes. *FYCO1* also mediates clearance of  
214  $\alpha$ -synuclein aggregates through a Rab7-dependent mechanism, overexpression reducing  
215 number of cell with  $\alpha$ -synuclein aggregates. Recently using single cell RNAseq authors  
216 identified a group of genes (*ATP6AP1*, *ATP6V1A*, *NPC1*, *RAB7A*, *CCDC22*, and *PIK3C3*)  
217 whose knockout induced shared transcriptional changes in cholesterol biosynthesis pathway<sup>13</sup>.  
218 They showed how the actual perturbation of the cholesterol biosynthesis pathway reduced viral  
219 infection. That furthermore reveals the links via RAB7. We hypothesize fewer pLOFs in *NPC1*  
220 to be present in cohorts of severe hospitalized patients with COVID-19. Niemann-Pick disease  
221 type C1 lipid storage disorder offers resistance to Ebola in cell line experiments and in  
222 homozygous recessive mice (*(Npc1-/-)*)<sup>18,19</sup>. Furthermore, bat species show selective sensitivity  
223 to Ebola versus Marburg viruses<sup>20</sup>. Our hypothesis is that people with certain lysosomal storage  
224 diseases may be resistant to one of these viruses. Along these lines there is suggestive evidence  
225 for this to be exactly the case. This is in line with a report by Sturley et al., authors propose that  
226 50 loci that in the homozygous state cause a lysosomal storage disorder, may account for  
227 divergent clinical outcomes in COVID-19.

228



229           Blocking or perturbing viral egress whether via Rab7, FYCO1 or other components may  
230 be a viable strategy to stop the proliferation of the virus reducing viral load. In the case of  
231 betacoronaviruses unconventional egress can be blocked by the Rab7 GTPase competitive  
232 inhibitor CID1067700<sup>11</sup> - compound potentially decreasing viral egress in a dose-dependent  
233 manner. Here we focused on downregulation of FYCO1: based on cell line expression with  
234 resulting potential candidates including indomethacin - a drug that has both anti-inflammatory  
235 and antiviral actions. Slowing viral spread by targeting regulators of lysosomal trafficking, by  
236 focusing on egress and double membrane vesicles may offer a therapeutics strategy for novel  
237 strain of betacoronaviruses.

238

239

240           The GWAS locus has led for further understanding of not only the more efficient egress  
241 leading to successful propagation of the viral particles but also to potential protective  
242 mechanisms and greater understanding of the heterogeneous clinical outcomes. We hence  
243 stipulate gain of function variants in *FYCO1* confer higher risk of infection with SARS and other  
244 betacoronaviruses. Downregulating or temporarily limiting, *FYCO1* activity may be protective.  
245 This susceptibility locus in fact highlights the potentially druggable cellular aspects of the host.

246

## 247 **Methods**

### 248 **Clinical Trial Information**

249 ODYSSEY is a double-blinded Phase 3 study with a planned randomization of a total of 300  
250 hospitalized severely ill COVID-19 patients to receive either tradipitant 85 mg bid or placebo for  
251 a total of up to 14 days or discharge (CONSORT Flowchart in S. File 1). The randomization is  
252 stratified by site with a block size of four. Inclusion criteria for the study comprised of: 1. Adults  
253 aged 18-90; 2. confirmed laboratory COVID-19 infection; 3. confirmed pneumonia by chest  
254 radiograph or computed tomography; 4. fever defined as temperature  $\geq 36.6$  °C armpit,  $\geq 37.2$  °C  
255 oral, or  $\geq 37.8$  °C rectal since admission or the use of antipyretics; 5. PaO<sub>2</sub> / FiO<sub>2</sub>  $\leq 300$ ; 6. in-  
256 patient hospitalization. Patients were to be followed for up to 28 days to record clinical  
257 outcomes. Patients' clinical progress was recorded on a 7 point clinical status ordinal scale  
258 defined as follows: 1- Death; 2- Hospitalized on mechanical ventilation or ECMO; 3-  
259 Hospitalized on non-invasive ventilation or high-flow oxygen supplementation; 4- Hospitalized

260 requiring supplemental oxygen; 5- Hospitalized not requiring supplemental oxygen, requiring  
261 continued medical care; 6- Hospitalized not requiring supplemental oxygen, not requiring  
262 continued medical care; 7- Not hospitalized.

263

## 264 **Human whole genome sequencing**

### 265 **Vanda Pharmaceuticals Inc. COVID-19 Cohort:**

266 WGS cohort consisted of 80 COVID-19 hospitalized patient samples and 1876 WGS controls.  
267 DNA was extracted from 200  $\mu$ l of whole blood using QIAamp blood mini kit and eluted into  
268 100  $\mu$ l volume in order to obtain 500 ng of DNA. Libraries were prepared by random  
269 fragmentation of DNA followed by adapter ligation using Illumina TruSeq adapters. Paired-end  
270 libraries 2x150 bp were sequenced on an Illumina NovaSeq6000 S4 with a target of 90Gb raw  
271 read depth per sample. The cohort was multi-ethnic and the age ranged from 35-87 for severe  
272 hospitalized COVID-19 cases (68% male, 32% female). Specifically the PC defined ancestry  
273 was as follows (African 9.8%, European 46.3%, Asian 4.9%, Hispanic 22% and other 17.1%).  
274 Furthermore, 16% of the cohort were patients hospitalized on mechanical ventilation or ECMO,  
275 13% deceased.

276 Both cases and controls were processed with the same bioinformatic pipeline for variant calling.  
277 Paired-end 150 $\times$ bp reads were aligned to the GRCh37 human reference (BWA-MEM v0.7.8)  
278 followed by Picard (MarkDuplicates) and processed with GATK best-practices workflow  
279 (GATK v3.5.0). The mean coverage was 35.8x. All high quality variants obtained from GATK  
280 were annotated. Annotations include variant effect predictions using VEP; allele frequencies  
281 from Gnomad; dbSNP 150 rsIDs; conservation scores from PhyloP, GERP, PhastCons; damaging  
282 effect predictions from Polyphen 2, SIFT and clinically relevant information from ClinVar. We  
283 removed samples with a discordance between self-declared and sequence-derived gender, we  
284 used KING for detection of related individuals and performed PCA for ancestry adjustment. The  
285 lead variant was in addition verified with genotyping (Supplementary Material). Logistic  
286 regression was conducted in PLINK, MATLAB. The analysis was corrected for PC 1-15, age  
287 and sex.

## 288 **Viral sequencing and genome assembly**

289 Sequencing was attempted on all samples with a positive RT-PCR assay result that had Ct <32  
290 using either a metagenomic approach described previously<sup>21</sup>, via IDT probe-capture<sup>22</sup>, or by  
291 amplicon sequencing with SWIFT library preparation. Libraries were sequenced on Illumina  
292 MiSeq or NextSeq instruments using 1x150 or 1x75 runs respectively. Consensus sequences  
293 were assembled using a custom bioinformatics pipeline [<https://github.com/proychou/hCoV19>]  
294 adapted for SARS-CoV-2 from previous work<sup>22, 23</sup>. Briefly, raw reads were trimmed to remove  
295 adapters and low quality regions using BBDuk and a k-mer based filter was used to pull out  
296 reads matching the reference sequence NC\_045512. Filtered reads were *de novo* assembled using  
297 SPAdes<sup>24</sup> and contigs were ordered against the reference using BWA-MEM. Gaps were filled by  
298 remapping reads against the assembled scaffold and a consensus sequence was called from this  
299 alignment using a custom script in R/Bioconductor.

300

## 301 **Cell culture and drug treatment**

302 Drugs screening was carried out, the same one as applied in our previous study<sup>25</sup>. The retinal  
303 pigment epithelia cell line, ARPE-19/HPV-16, was chosen to establish a database of drug  
304 profiles because of its non-cancerous, human origin, with a normal karyotype. It can also be  
305 easily grown as monolayer in 96-well plates. Compounds were obtained from Sigma (St. Louis,  
306 MO) or Vanda Pharmaceuticals (Washington, DC). Cells were aliquoted on 96-well plates  
307 (~2×10<sup>5</sup> cells/well) and incubated for 24 h prior to providing fresh media with a drug, or the  
308 drug vehicle (water, dimethyl sulfoxide, ethanol, methanol, or phosphate-buffered saline  
309 solution). Drugs were diluted 1000 fold in buffered in Dulbecco's Modified Eagle Medium:  
310 Nutrient Mixture F-12 (D-MEM/F-12) culture medium (Invitrogen, Carlsbad, CA) containing  
311 nonessential amino acids and 110 mg/L sodium pyruvate. In these conditions, no significant  
312 changes of pH were expected, which was confirmed by the monitoring of the pH indicator  
313 present in the medium. A final 10 μM drug concentration was chosen because it is believed to fit  
314 in the range of physiological conditions<sup>25</sup>. Microscopic inspection of each well was conducted at  
315 the end of the treatment to discard any samples where cells had morphological changes  
316 consistent with apoptosis. We also verified that the drug had not precipitated in the culture  
317 medium.

318

319 **Gene expression**

320 Cells were harvested 24 h after treatment and RNA was extracted using the RNeasy 96 protocol  
321 (Qiagen, Valencia, CA). Gene expression for 22,238 probe sets of 12,490 genes was generated  
322 with U133A2.0 microarrays following the manufacturer's instructions (Affymetrix, Santa Clara,  
323 CA). Drugs were profiled in duplicate or triplicate, with multiple vehicle controls on each plate.  
324 A total of 708 microarrays were analyzed including 74 for the 18 antipsychotics, 499 for the  
325 other 448 compounds, and 135 for vehicle controls. The raw scan data were first converted to  
326 average difference values using MAS 5.0 (Affymetrix). The average difference values of both  
327 treatment and control data were set to a minimum of 50 or lower. For each treatment category,  
328 all probe sets were then ranked based on their amplitude, or level of expression relative to the  
329 vehicle control (or the average of controls was selected when more than one was used).  
330 Amplitude was defined as the ratio of expression  $(t-v) / [(t+v) / 2]$  where t corresponds to  
331 treatment instance and v to vehicle instance. Each drug group profile was created using our novel  
332 Weighted Influence Model, Rank of Ranks (WIMRR) method which underscores the rank of  
333 each probe set across the entire gene expression profile rather than the specific change in  
334 expression level. WIMRR takes the average rank of each probe set across all of the members of  
335 the group and then reranks the probe sets from smallest average rank to largest average rank. A  
336 gene-set enrichment metric based on the Kolmogorov– Smirnov (KS) statistic. Specifically, for a  
337 given set of probes, the KS score gives a measure of how up (positive) or down (negative) the set  
338 of probes occurs within the profile of another treatment instance.

339

340 **Declarations**

341 **Funding:** Vanda Pharmaceuticals Inc.

342 **Competing Interests:** SPS,BPP,MHP are employees of Vanda Pharmaceuticals.

343 **Ethical Approval:** Reviewed and approved by Advarra IRB; Pro00043096

344

345

346

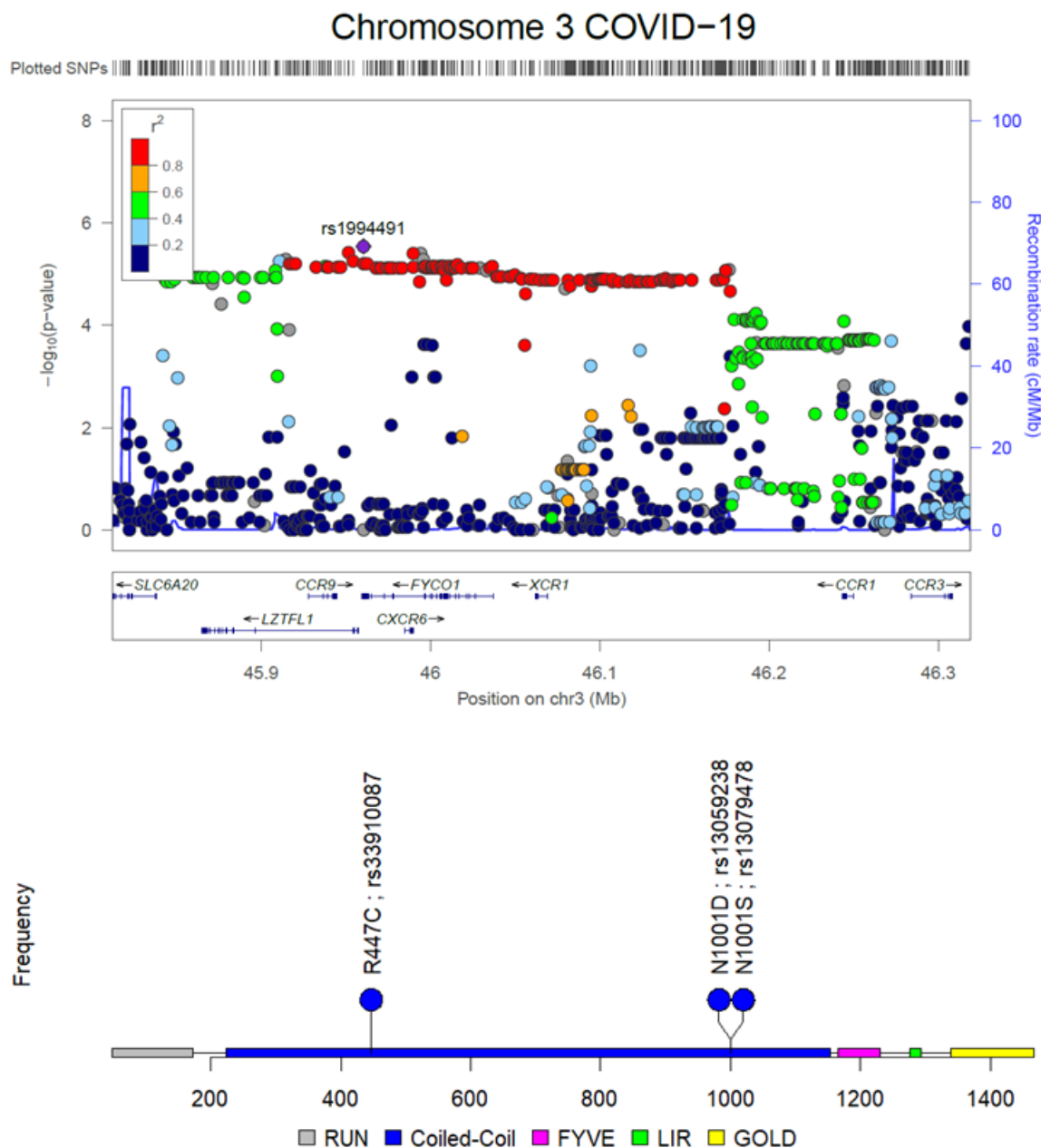
347 **References**

- 348 1. Zhu, N. *et al.* A Novel Coronavirus from Patients with Pneumonia in China, 2019. *New*  
349 *England Journal of Medicine* **382**, 727–733 (2020).
- 350 2. Zhou, F. *et al.* Clinical course and risk factors for mortality of adult inpatients with  
351 COVID-19 in Wuhan, China: a retrospective cohort study. *The Lancet* **395**, 1054–1062  
352 (2020).
- 353 3. Ganna, A., Unit, T. G. & General, M. The COVID-19 Host Genetics Initiative , a global  
354 initiative to elucidate the role of host genetic factors in susceptibility and severity of the  
355 SARS-CoV-2 virus pandemic. 715–718 (2020). doi:10.1038/s41431-020-0636-6
- 356 4. Genomewide Association Study of Severe Covid-19 with Respiratory Failure. *New*  
357 *England Journal of Medicine* **383**, 1522–1534 (2020).
- 358 5. Pairo-Castineira, E. *et al.* Genetic mechanisms of critical illness in Covid-19. *medRxiv* **17**,  
359 25 (2020).
- 360 6. Karczewski, K. J. *et al.* Variation across 141,456 human exomes and genomes reveals the  
361 spectrum of loss-of-function intolerance across human protein-coding genes. *bioRxiv*  
362 531210 (2019). doi:10.1101/531210
- 363 7. Zeberg, H. & Pääbo, S. The major genetic risk factor for severe COVID-19 is inherited  
364 from Neanderthals. *Nature* (2020). doi:10.1038/s41586-020-2818-3
- 365 8. Lonsdale, J. *et al.* The Genotype-Tissue Expression (GTEx) project. *Nature Genetics* **45**,  
366 580–585 (2013).
- 367 9. Zhang, J., Lan, Y. & Sanyal, S. Membrane heist□: Coronavirus host membrane  
368 remodeling during replication. (2020).
- 369 10. Pankiv, S. *et al.* *FYCO1* is a Rab7 effector that binds to LC3 and PI3P to mediate  
370 microtubule plus end - Directed vesicle transport. *Journal of Cell Biology* **188**, 253–269  
371 (2010).
- 372 11. Ghoush Amit Kumar Mandal , Paulami Dam , Octavio L. Franco , Hanen Sellami ,  
373 Sukhendu Mandal , Gulden Can Sezgin , Kinkar Biswas , Partha Sarathi Nandi, I. O. b-  
374 Coronaviruses Use Lysosomes for Egress Instead of the Biosynthetic Secretory Pathway.  
375 *Cell* 19–21 (2020).
- 376 12. Saridaki, T. *et al.* *FYCO1* mediates clearance of  $\alpha$ -synuclein aggregates through a Rab7-  
377 dependent mechanism. *Journal of Neurochemistry* **146**, 474–492 (2018).

- 378 13. Daniloski, Z. *et al.* Identification of required host factors for SARS-CoV-2 infection in  
379 human cells. *Cell* 1–14 (2020). doi:10.1016/j.cell.2020.10.030
- 380 14. Reggiori, F., de Haan, C. A. M. & Molinari, M. Unconventional use of LC3 by  
381 coronaviruses through the alleged subversion of the ERAD tuning pathway. *Viruses* **3**,  
382 1610–1623 (2011).
- 383 15. Singer, J., Gifford, R., Cotten, M. & Robertson, D. CoV-GLUE: A Web Application for  
384 Tracking SARS-CoV-2 Genomic Variation. *Preprints* 2020060225 (2020).  
385 doi:10.20944/PREPRINTS202006.0225.V1
- 386 16. Elbe, S. & Buckland-Merrett, G. Data, disease and diplomacy: GISAID’s innovative  
387 contribution to global health. *Global Challenges* **1**, 33–46 (2017).
- 388 17. Grubaugh, N. D., Hanage, W. P. & Rasmussen, A. L. Making Sense of Mutation: What  
389 D614G Means for the COVID-19 Pandemic Remains Unclear. *Cell* **182**, 794–795 (2020).
- 390 18. Withrock, I. C. *et al.* Genetic diseases conferring resistance to infectious diseases. *Genes*  
391 *& Diseases* **2**, 247–254 (2015).
- 392 19. Takadate, Y. *et al.* Niemann-Pick C1 Heterogeneity of Bat Cells Controls Filovirus  
393 Tropism. *Cell Reports* **30**, 308–319.e5 (2020).
- 394 20. Haines, K. M., Vande Burgt, N. H., Francica, J. R., Kaletsky, R. L. & Bates, P. Chinese  
395 hamster ovary cell lines selected for resistance to ebolavirus glycoprotein mediated  
396 infection are defective for NPC1 expression. *Virology* **432**, 20–28 (2012).
- 397 21. Greninger, A. L. *et al.* Rapid metagenomic next-generation sequencing during an  
398 investigation of hospital-acquired human parainfluenza virus 3 infections. *Journal of*  
399 *Clinical Microbiology* **55**, 177–182 (2017).
- 400 22. Greninger, A. L. *et al.* Ultrasensitive Capture of Human Herpes Simplex Virus Genomes  
401 Directly from Clinical Samples Reveals Extraordinarily Limited Evolution in Cell  
402 Culture. *mSphere* **3**, 1–12 (2018).
- 403 23. Greninger, A. L. *et al.* Proteomic Reannotation of Human Herpesvirus 6. 1–17 (2018).
- 404 24. Bankevich, A. *et al.* SPAdes: A new genome assembly algorithm and its applications to  
405 single-cell sequencing. *Journal of Computational Biology* **19**, 455–477 (2012).
- 406 25. Polymeropoulos, M. H. *et al.* Common effect of antipsychotics on the biosynthesis and  
407 regulation of fatty acids and cholesterol supports a key role of lipid homeostasis in  
408 schizophrenia. *Schizophrenia Research* **108**, 134–142 (2009).

409 **Figure Legend**

410 **Figure 1.** Figure 1A depicts the coding variants detected in the region association with severity  
 411 of COVID-19 infection in FYCO1 gene. Figure 1B is a locus zoom of the entire significant  
 412 chromosome 3 region associated with severe COVID-19 based on a whole genome sequencing  
 413 analysis.  
 414



415

416

417

418

419